23 ACCRETION

23.1 *Useful references*

- Murray & Dermott, Ch. 3
- Choudhuri, Secs. 4.5.1, 5.6
- Hansen, Kawaler, and Trimble, Sec. 2.13

Much of our empirical knowledge of neutron stars and black holes comes from **accretion**: the flow of material from some object (usually a star) onto another. Accretion is a ubiquitous process in astrophysics, contributing to the formation and growth of planets ($< 10^{-3}M_\odot$), stars ($\sim M_\odot$), stellar remnants such as white dwarfs, neutron stars and black holes ($\lesssim 40M_\odot$), and even the supermassive black holes that lie at the centers of galaxies ($10^6 - 10^9 M_\odot$).

23.2 *Lagrange Points and Equilibrium*

Our first goal is to identify the points of equilibrium in a two-body binary system with orbital period P. Imagine a test particle (e.g., an atom of potentially accretable gas) near the binary: what forces act on it? To answer this we examine the system in a frame co-rotating with the binary, as sketched in Fig. 53. We have two objects with masses $m_1 > m_2$,

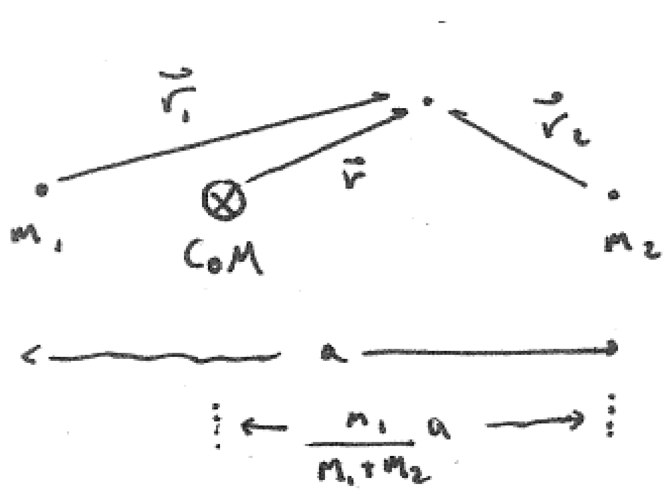

Figure 53: Schematic view of a coordinate frame co-rotating with a binary. "CoM" indicates the center of mass.

total mass M, mass ratio $q = m_1/m_2$, and a systemic angular velocity

(588)
$$\vec{\Omega} = \frac{2\pi}{P}\hat{z}$$
(589)
$$= \left(\frac{GM}{a^3}\right)^{1/2}\hat{z}$$

We expect to find a zone of influence near each body in the binary, such that our test particle will remain near that body. Any material inside this zone will stay on or near its dominating body; any material outside the zone will not be bound and could accrete onto the other object. For two stationary masses the effective potential would merely be the sum of their gravitational wells; the key difference here is that since we are considering the test particle within a rotating (non-inertial) reference frame, we must include a fictitious centrifugal force as well. In this **Roche potential**, we then have

(590) $$\psi_R(\vec{r}) = -G\frac{m_1}{r_1} - G\frac{m_2}{r_2} - \frac{1}{2}\Omega^2 r^2.$$

Note that the Roche potential, including only the centrifugal term, is just fine for considering equilibrium points (at which our test particle would be stationary). To consider dynamics and particle trajectories (i.e. nonzero velocities), we would also need to consider the (also fictitious)

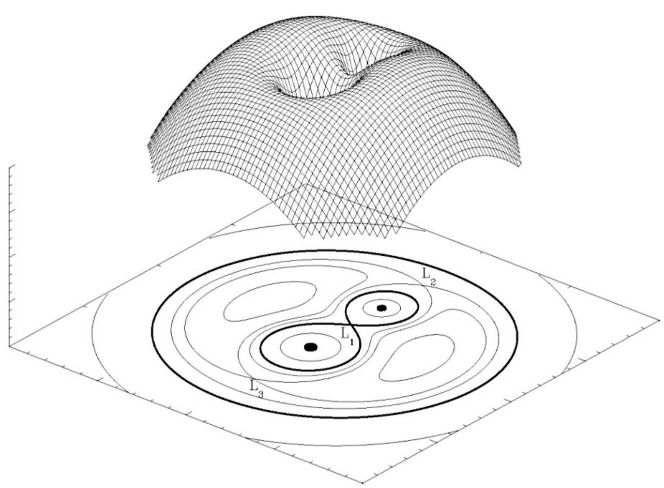

Figure 54: Roche potential (Eq. 590) as a surface plot (above) and as contour plot (below). Lagrange points 1–3 are noted; points 4 and 5 would be to either side of the "figure eight."

Coriolis term:

(591) $\vec{F}_{\text{Cor}} = 2m\vec{v} \times \vec{\Omega}$.

But so long as $v = 0$, we can neglect it.

Fig. 54 depicts the Roche potential as both a 3D mesh surface plot and a 2D contour plot. Note several key features:

- The gravitational well of each star shows up prominently for small $\vec{r}_1$ and $\vec{r}_2$. At large r, the centrifugal term dominates.
- If we take a cross-sectional cut along the line connecting the masses, ψ_R shows three local maxima. These are the first three **Lagrange Points** (actually found by Euler). L_1 is between the two objects (it is *not* the center of mass), L_2 is outside the low-mass object, and L_3 is outside the high-mass object.
- Expanding from the cross-section to the full 2D plane, there are two local maxima to each side: these are the final Lagrange points, L_4 and L_5. Furthermore, note that $L_1 - L_3$ are actually saddle points, and not truly local maxima.

All five of the Lagrange points can be identified as equilibrium points by setting

$$\vec{\nabla}\psi_R = 0.$$

As is apparent from Fig. 54, in the Roche description none of these five points appear to be truly stable equilibria. As noted above, this is because we have neglected Coriolis forces. When these are included $L_1 - L_3$ remain at least mildly unstable (or worse), but spacecraft can still maintain orbits around these points with only minimal use of thrusters.

Points L_4 and L_5 turn out to be true equilibria: given a small perturbation from those points, the Coriolis force will keep the test particle in funny-looking orbits around one or the other of these two points. If given a relatively small perturbation the test particle will exhibit so-called **tadpole orbits**, oscillating around L_4 or L_5 with a greater displacement toward L_3 than toward L_2. Thousands of asteroids are seen librating around Jupiter's L_4 and L_5 points; such objects are often terms **Trojans**. If given sufficient impetus, the test particle can be sent into a **horseshoe orbit**, wherein it oscillates around most of the system (as viewed from within the rotating frame). An object is a horseshoe orbit is less tightly bound and ranges over a much broader range of parameter space; nonetheless numerous such objects are also known.

23.3 *Roche Lobes and Equipotentials*

In this rotating reference frame, a star in equilibrium will still satisfy the equation of hydrostatic equilibrium. Now we no longer have spherical symmetry, so our 3D equivalent of Eq. 192 is

$$\vec{\nabla} P = -\rho \vec{g}_{\text{eff}} = -\rho \vec{\nabla} \psi_R. \tag{592}$$

This means that the contours of ψ_R shown in Fig. 54 correspond to surfaces of constant pressure.

One often speaks of a Roche lobe radius – i.e., the radius of a sphere with the same volume as the Roche lobe. For star one, an approximation good to 1% is

$$\frac{R_1}{a} = \frac{0.49 q^{2/3}}{0.6 q^{2/3} + \ln(1 + q^{1/3})}. \tag{593}$$

If $q \ll 1$, then an even simpler approximation is

$$\frac{R_1}{a} \approx \frac{1}{2} q^{1/3}. \tag{594}$$

In particular, the outermost layer of the star will itself be shaped like one of these contours; in binary-speak, we say that the star only partially fills its **Roche lobe.** If neither star completely fills its Roche lobe, then we have a **detached binary**. As we consider a larger and larger star (of constant mass), the star will become increasingly almond-shaped. Eventually it will become so large that it completely fills its Roche lobe; if it becomes any larger, some of its material will fall through the narrow neck of the hourglass and enter the potential well of the other mass. An astronomer would say that the star is overflowing its Roche lobe; we then have a **semi-detached binary** (Algol is a classic example). If both stars fill their Roche lobes, then the "binary" is now a dumbbell-shaped **contact binary** rotating at the Keplerian period. In the most extreme case, a **common-envelope binary**, the cores of two stars can orbit together deep inside of a single, common envelope that now may rotate at a speed wholly unrelated to the Keplerian period. Regardless of the type of overflow, substantial mass transfer will occur and so the stellar evolution of the stars involved can be significantly affected.

23.4 *Roche Lobe Overflow*

When Roche lobe overflow occurs, material spills over at L_1 and falls down the companion's gravity well. Roche Lobe overflow can dramatically complicate stellar evolution in a binary system. Given a binary composed of two main-sequence stars, we might naively expect the smaller lobe to overflow first. But the more massive star (with the larger Roche lobe) will have a shorter life and will evolve first into a giant.

At this point, something interesting happens: as the star (say, m_1) expands and mass transfer begins, by Eq. 594 its Roche radius will shrink. The combined effect is to accelerate mass transfer; until in some cases m_2 may become more massive than m_1. Material may even slosh back and forth between the two objects a time or two, but before too long one object or another will end its stellar life, as either a white dwarf, neutron star, or black hole.

23.5 *Accretion Disks*

Once our binary contains a compact stellar remnant, if the binary separation and mass ratio are right then one last phase of mass transfer can occur. When overflow occurs in a system with a compact object (WD, NS, or BH; call it m_2), the material has a long way to fall. It is pushed over the brink by the unbalanced pressure at L_1, and falls down toward m_2 with a velocity $v \approx c_s \sim 10s$ km s^{-1} — much smaller than the orbital speeds of ~ 100 km s^{-1}. When m_2 had a large radius this material would easily hit its target, but in this later phase of evolution the target is far smaller.

Now, the overflowing gas heads down, down toward m_2 — but all the while, the $\vec{v} \times \vec{\Omega}$ Coriolis force is steadily acting on the material, causing it to veer away from a direct path. The combined potential leads to the matter entering into an orbit around m_2, with the material's trajectory passing through its former position and smashing into the material that was coming along behind it.

Shock heating sets in where the infalling stream impacts the growing disk of matter, converting bulk kinetic energy into heat. Radiation can try to cool the hot, shocked material but it can't transport much angular momentum: so the accreted material ends up in a circular **accretion disk.**

Further evolution of the disk is set by its ability to transport mass inward through the disk while simultaneously moving angular momentum outward – these parameters are set in turn by the viscosity of the disk. Each concentric annulus of material in the disk wants to travel at a slightly different Keplerian speed. Very close to m_2 at the center of our accretion disk, orbits are determined solely by m_2 and so travel at the Keplerian angular velocity

$$(595)\quad \Omega_K(r) = \frac{v}{r} = \sqrt{\frac{GM}{r^3}}.$$

Meanwhile, the angular momentum per unit mass is

$$(596)\quad \ell(r) = rv = r^2\Omega_K = \sqrt{GMr}.$$

So as we go outward through successive annuli of the disk, Ω decreases but ℓ increases. These rings, rotating at different speeds, are coupled by viscosity – this effectively acts like friction. So each interior ring tries to speed up the rotation of its exterior neighbor, sending angular momentum outward and pushing out that exterior neighbor. At the same time, the ring interacts viscously with the next ring inward, trying to slow it down and so causing it to fall inward. The net effect is that the disk